

Analysis of Long Period Events in January 2024 on the Reykjanes Peninsula, Iceland

Report for Volcanoseismology, SoSe 2024

Module: MGPW02

Student's Name LEAH REES

Matriculation Number: 825231

Supervisor: PROF. DR. EVA EIBL

Submission Date: 01. August 2024

Table of Contents

1 Abstract	2
2 Introduction	2
2.1 Chronology of Volcanic Activity 2021-2024	3
3 Data Analysis and Interpretation	4
3.1 Waveform and Frequency Analysis of Initial Catalog	5
3.2 Particle Motion	6
3.3 Back Azimuth	7
3.4 Overview of the Events in Time	8
3.5 Cross Correlation	9
4 Results and Discussion	10
5 References	11

1 Abstract

This study investigates Long-Period (LP) seismic events associated with volcanic activity on the Reykjanes Peninsula, Iceland, during January 2024. Utilizing seismic data from stations SAND and SVA, an initial catalog of 43 potential LP events was established using a bandpass filter between 0.5 and 2 Hz. Detailed analysis, including waveform and frequency content examination, reduced this to 27 confirmed LP events. Particle motion analysis revealed complex patterns, with significant vertical polarization indicating the characteristic behavior of LP events. Rotational sensor data provided back azimuths predominantly around 180 degrees for the events, suggesting potential sources near Gríndavík. Temporal distribution of events highlighted a clustering around January 14th, correlating with the eruption's onset at 07:57 UTC, indicating pre-eruptive fluid movements. Cross-correlation analysis of a template event identified 39 events, reinforcing the pre-eruptive concentration of seismic activity. This comprehensive analysis highlights the role of fluid dynamics in generating LP seismicity.

2 Introduction

The Figure 1 consists of two maps illustrating volcanic and tectonic features of the Reykjanes peninsula of Iceland (Troll et al., 2024). The first map (a) is a regional map showing the southwestern part of Iceland, highlighting various volcanic zones, tectonic features, as well as volcanic systems. A black dashed line represents the plate boundary with an arrow indicating the direction of plate movement at a rate of 9 mm/year. Further, major settlements such as Reykjavík, Keflavík, Vogar, Reykjanesbær, and Grindavík are also marked.

The second map (b) provides a detailed view of a specific area within the Reykjanes Peninsula, focusing on recent volcanic activity. This map highlights recent eruptions with different colors: The Fagradalsfjall Fires (2021-2023) in yellow, green, and blue, and the more recent Sundhnúkur Fires (2023-24) in red. The town of Grindavík is located near the more recent eruptions, which is also the location of the January 2024 eruption analyzed in this report.

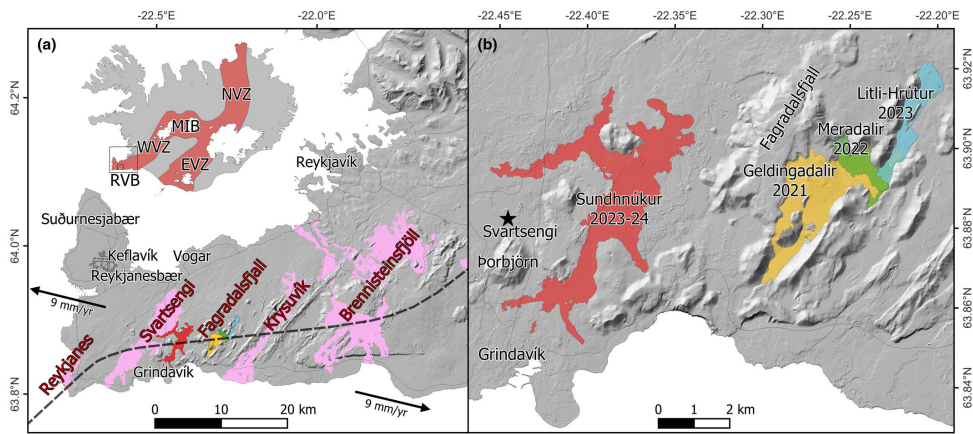


Figure 1: Map of Iceland's volcanic systems, highlighting the different volcanic zones including the Reykjanes Peninsula (left plot), with specific areas of recent volcanic activity marked for 2021, 2022, 2023, and 2023-2024 near Svartsengi and Grindavík (right map) (Troll et al., 2024)

The various types of seismic events observed at volcanoes, such as Volcano-Tectonic (VT) earthquakes, Long-Period (LP) events, and tremor, arise from the complex interplay of gases, fluids, and solids within the volcanic system (Chouet and Matoza, 2013).

LP seismicity, characterized by frequencies typically ranging from 0.5 to 5 Hz as can be seen in Figure 2 (from Sciotto et al., 2022), do have an emergent P-Wave and no distinct S-Wave. They are thought to

primarily originate from fluid-related processes such as the formation and collapse of gas bubbles, as well as the movement of fluids into cracks or conduits within the volcano (Sciutto et al., 2022; Chouet, 1996). Additionally, shear failure within the volcanic structure can also generate LP events, contributing to the diverse nature of this seismic activity.

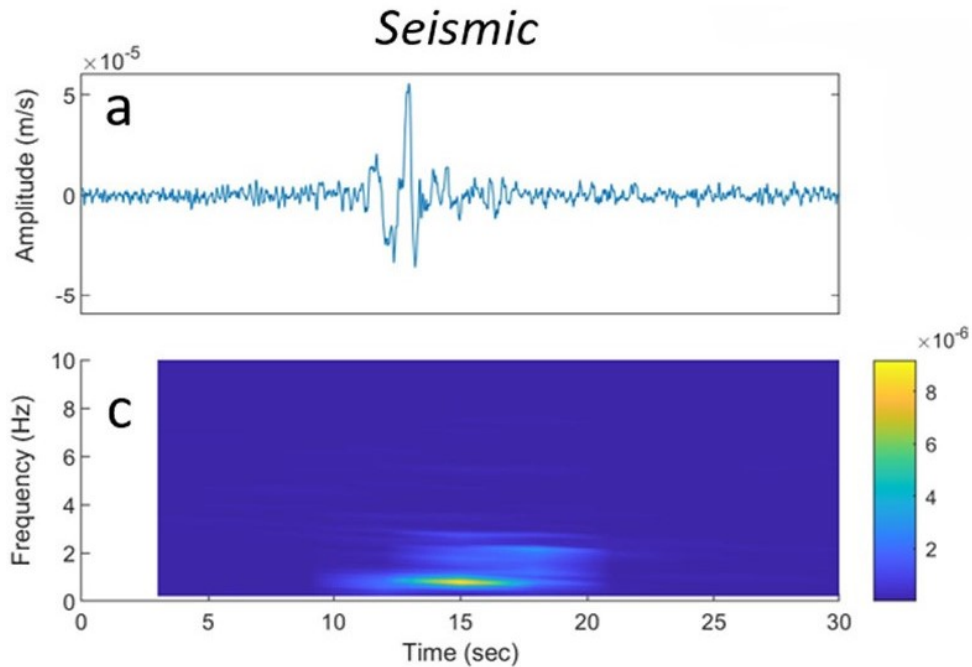


Figure 2: Seismogram (a) and spectrogram (c) of an example LP event recorded at Mt. Etna (modified Figure by Sciutto et al., 2022)

2.1 Chronology of Volcanic Activity 2021-2024

Starting on March 19, 2021, after 781 years of rest, the Geldingadalir eruption began on the Fagradalsfjall peninsula in South-West Iceland (Troll et al., 2024). Following that eruption were the Geldingadalir eruption in 2022 and the Litli-Hrútur eruption in 2023. All three eruptions belong to the Fagradalsfjall Fires. This eruption sequence proceeds into the ongoing Sundhúkur Fires that started in December 2023. The Sundhúkur Fires are located between the Svartsengi and the Fagradalsfjall volcanic systems, just north of Grindavík (see Figure 1). They were preceded by an increase in seismic activity in October 2023, which led to an earthquake swarm on November 10, 2023. During this swarm, several grabens were formed north of Grindavík.

After the earthquake swarm, continuous land uplift, likely due to magma intrusion, eventually led to the first eruption of the Sundhúkur Fires on December 18, 2023 (Troll et al., 2024). Subsequent eruptions occurred in January, February, March to May, and May to June of 2024, continuing this eruption sequence. All the eruptions are roughly located north of Grindavík (see Figure 1).

As this report focuses on the LP Events during January 2024, a more detailed introduction to that month will be provided.

At the start of January 2024, there was an earthquake swarm (IMO). On January 9, 2024, a land uplift of 5 mm per day was recorded, bringing the land to be 5 cm above its pre-dike intrusion level in November 2023. This uplift lasted until 3:00 AM on January 14, when there was a sharp increase in seismic activity North of Grindavík. The second eruption of the Sundhúkur Fires began on January 14, 2024, at 7:57 UTC.

Two new fissures opened during that eruption (see Figure 3) (IMO). While the fissure from the December eruption was further north, the fissures that opened during the January eruption were closer to the city,

with one fissure just 900 meters north of Grindavík.

After the eruption ended on January 16, 2024, a decrease in seismicity was observed in the seismic data (IMO). However, the magma conduit beneath Grindavík appeared to expand further. Moreover, land kept uplifting after the eruption, reaching a rate of 8 mm per day by January 25, 2024. Despite the uplift, seismic activity remained low until the end of January.

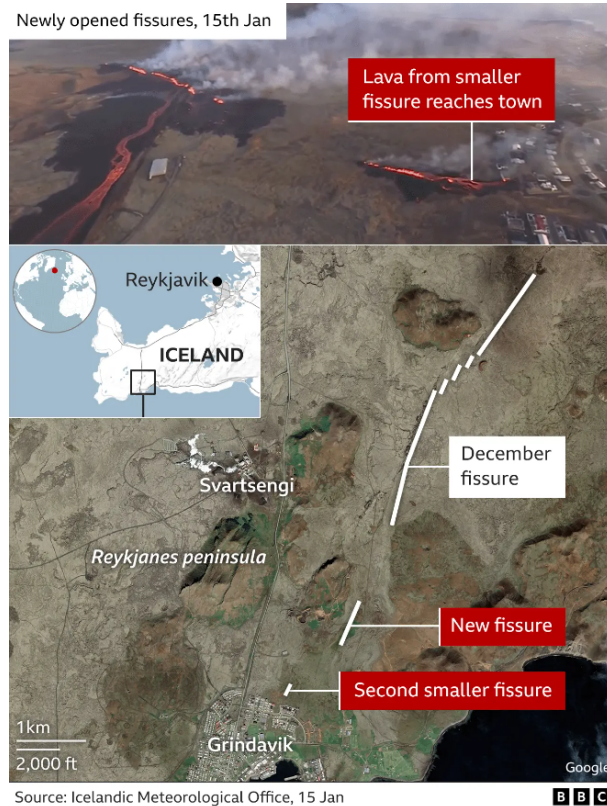


Figure 3: Map showing recent volcanic activity on the Reykjanes Peninsula, highlighting new fissures from January 15th, as well as fissures from December, near Grindavík (BBC News, 2024)

3 Data Analysis and Interpretation

During this analysis, the seismic data from January 2024 from two stations, SAND and SVA, was utilized. Mainly, the data from the broadband sensor at the SAND station was used, while the data from the rotational sensor at the SVA station was only employed for the backazimuth calculation. The broadband sensor data from SAND was detrended, tapered, and velocity instrument corrected. Additionally, various bandpass filters were applied to enhance the clarity of the signals as needed.

To compile an initial catalog of potential LP events, a first example was identified in the data. This event served as a reference for setting the parameters for the STA/LTA Detector in Snuffler (Heimann et al., 2017). The detector was configured with a bandpass filter ranging from 0.5 to 2 Hz, as detected events above 2 Hz were predominantly VT events. The other chosen parameters are a 12-second STA window, a 48-second LTA window, and a detection threshold of 0.7. After carefully reviewing the selected events and picks, the initial catalog contained 43 potential LP events for January.

Subsequent steps involved further analysis of these events to confirm their status as LP events. Seismograms and spectrograms were utilized to assess their characteristics. The events that remained in

the catalog after this inspection were scrutinized in terms of their occurrence time in January, particle motion, and Backazimuth. Additionally, cross-correlation analysis using Obspy (Beyreuther et al., 2010) was performed to evaluate the completeness of the catalog and to compare the effectiveness of the two methods used to compile it.

3.1 Waveform and Frequency Analysis of Initial Catalog

In this chapter, I will conduct a detailed analysis of the events from the initial catalog by plotting their waveforms and frequency contents. The waveforms are examined using seismograms, with the upper seismogram bandpass filtered from 5-15 Hz, which corresponds to the expected frequency range of most VTEs (Wassermann, 2012), and the lower seismogram bandpass filtered from 0.5-5 Hz. Since this is a check for LP events, all the energy should be in the lower seismogram, while the upper seismogram should only contain background noise.

Figure 4 displays the waveforms of two selected events. The first event, shown in Figure 4a, exhibits some energy in the lower seismogram, however, the upper seismogram shows significant energy at the start of the event. On the other hand, Figure 4b shows an event with barely any energy in the 5-15 Hz bandpass filtered seismogram, while all the energy of the event is contained in the lower 0.5-5 Hz filtered seismogram. To ensure accurate event classification, this waveform inspection was conducted alongside an analysis of the frequency content.

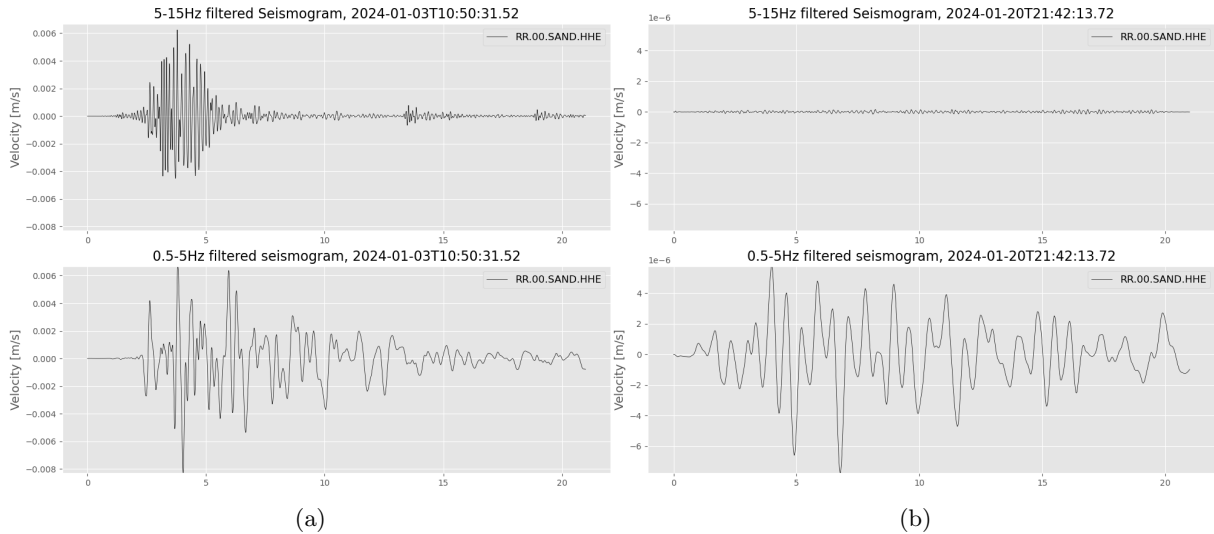


Figure 4: Seismograms of two example events from the initial catalog, upper Figures bandpass filtered 5-15 Hz, lower Figures bandpass filtered 0.5-5 Hz

The frequency content of the events was examined by plotting their spectrograms. Each spectrogram consists of two subplots: the upper spectrogram is unfiltered to provide a comprehensive view of the frequency content, while the lower spectrogram is bandpass filtered from 0.5-5 Hz. The same events from Figure 4 were used for this visualization in Figure 5. Once again, the first event in Figure 5a shows some energy above the LPE frequency band (see chapter 2). In contrast, the second event in Figure 5b has all its energy content below 5 Hz, whether filtered or unfiltered.

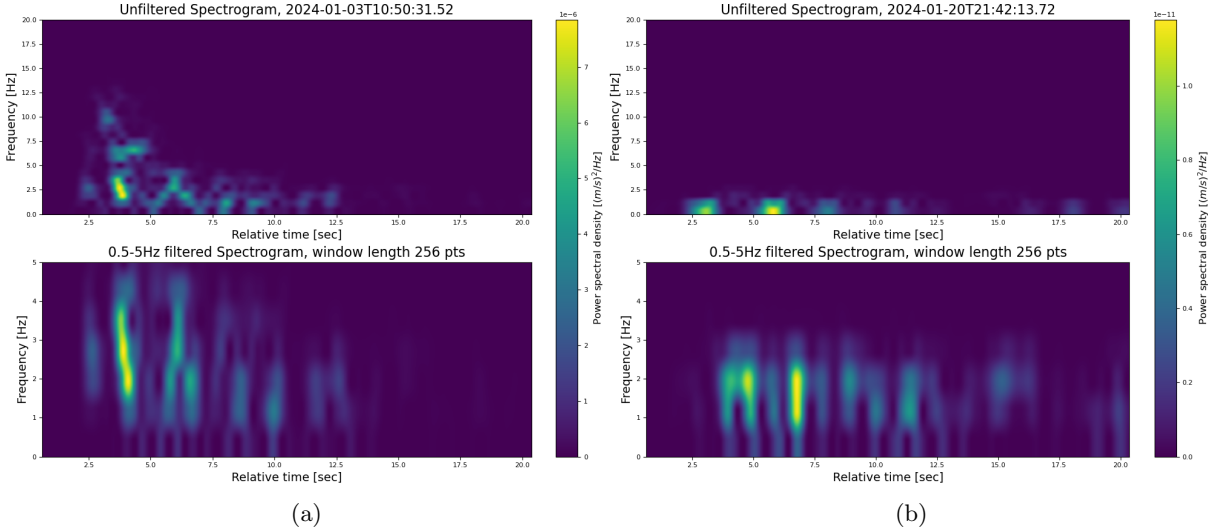


Figure 5: Spectrograms of two example events from the initial catalog, upper Figures unfiltered, lower Figures bandpass filtered 0.5-5 Hz

After plotting the seismograms and spectrograms for all the events in the initial catalog, each event was individually analyzed using these Figures. If an event exhibited the characteristics of a possible LPE in both the seismogram and spectrogram, it was added to the revised event catalog. The revised catalog contains 27 events.

3.2 Particle Motion

In order to have a better understanding of the particle motion of the first arrivals of the events, a more furrow analysis is necessary. Therefore, the plots represent the first second of each event, with the data trimmed to show this initial period after the arrival.

The Figure 6 displays three particle motion plots from a seismic event that occurred on January 14, 2024, at 05:16:14 UTC. This event has been chosen as a representative event for the events in the secondary event catalog. Each plot represents the motion in a different plane. The left plot shows the particle motion in the HHE-HHN plane, where the horizontal east (HHE) component is on the x-axis and the horizontal north (HHN) component is on the y-axis. The trajectory in this plot shows a looping pattern, indicating complex motion with significant contributions from both horizontal components.

The middle plot represents the particle motion in the HHZ-HHN plane, with the vertical (HHZ) component on the x-axis and the HHN component on the y-axis. Here, the trajectory is more elongated vertically, suggesting a stronger contribution from the vertical component compared to the horizontal north component.

The right plot illustrates the particle motion in the HHZ-HHE plane, where the HHZ component is on the x-axis and the HHE component is on the y-axis. The trajectory in this plot appears more complex than the particle motion in the HHZ-HHN plane, yet, the wave is still mainly polarized in the vertical direction.

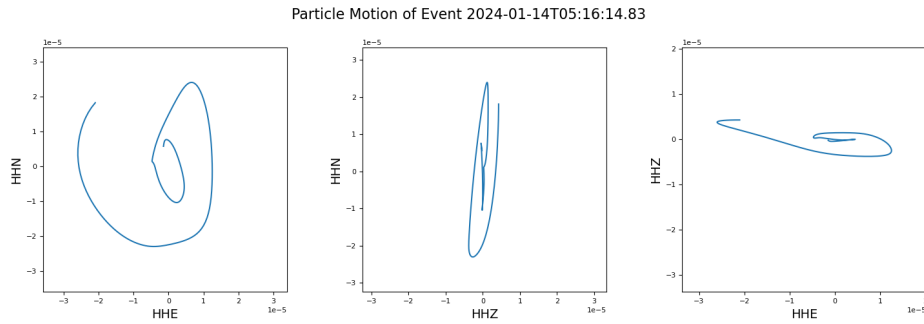


Figure 6: Particle Motion of an example event from the revised catalog showing the first second of recorded particle motion of the 3-component station SAND.

3.3 Back Azimuth

Using data from the rotational sensor at the SVA station, the back azimuth was calculated to determine the direction of incoming seismic events. For this analysis, the event at 06:16:46 UTC was selected. Since this is the only analysis utilizing rotational sensor data from the SVA station, the data underwent preprocessing, including detrending, tapering, and applying a 1-3 Hz bandpass filter. The instrument response was not removed during this process.

The Figure 7 presents a series of plots related to seismic rotation rates and back azimuths recorded on January 14, 2024, starting at 06:16:40 UTC with the chosen event starting at 06:16:46 UTC.

The first plot, labeled "Rotation rate E," shows the rotation rate in the east direction over time. The second plot, labeled "Rotation rate N," depicts the rotation rate in the north direction. The third plot shows the back azimuth, which is the direction from which the seismic waves are arriving, measured in degrees. The y-axis ranges from 0 to 360 degrees, and the x-axis represents time in seconds. The plot shows the back azimuth values as a function of time. The back azimuth remains relatively stable around 240 degrees for most of the period, with some minor variations. The plot also includes a small histogram on the right side, summarizing the distribution of back azimuth values over the time period.

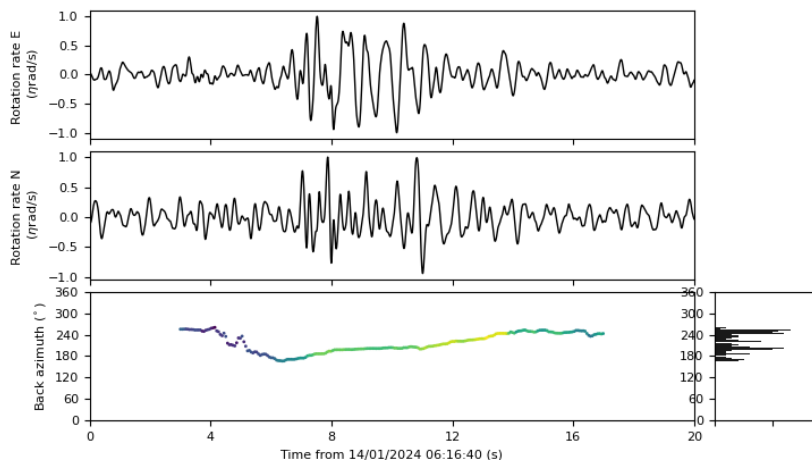


Figure 7: Rotational sensor data from the SVA station on January 14, 2024, showing rotation rates in the east (upper plot) and north directions (middle plot) and the calculated back azimuth (lower plot and histogram) for a representative event at 06:16:46 UTC

The Figure illustrates that the background noise predominantly originates from around 240 degrees, which could be attributed to sources such as the ocean or the Svartsengi and orbjörn areas. However, during the event, the backazimuth shifts to approximately 180 degrees, directly south of the SVA station. This direction encompasses not only Gríndavík but also the fissures that opened in January 2024 and December 2023, as well as the graben that formed in November 2023.

3.4 Overview of the Events in Time

This chapter delves into a more detailed analysis of the events over time. For this purpose, several histograms have been created. One histogram illustrates the overall distribution of events throughout the entire month of January. Conversely, the revised event catalog primarily contains events concentrated on January 14th, with only two additional events occurring on January 20th and January 27th. Consequently, a more detailed histogram focusing on January 14th was generated. Both plots are shown in Figure 8.

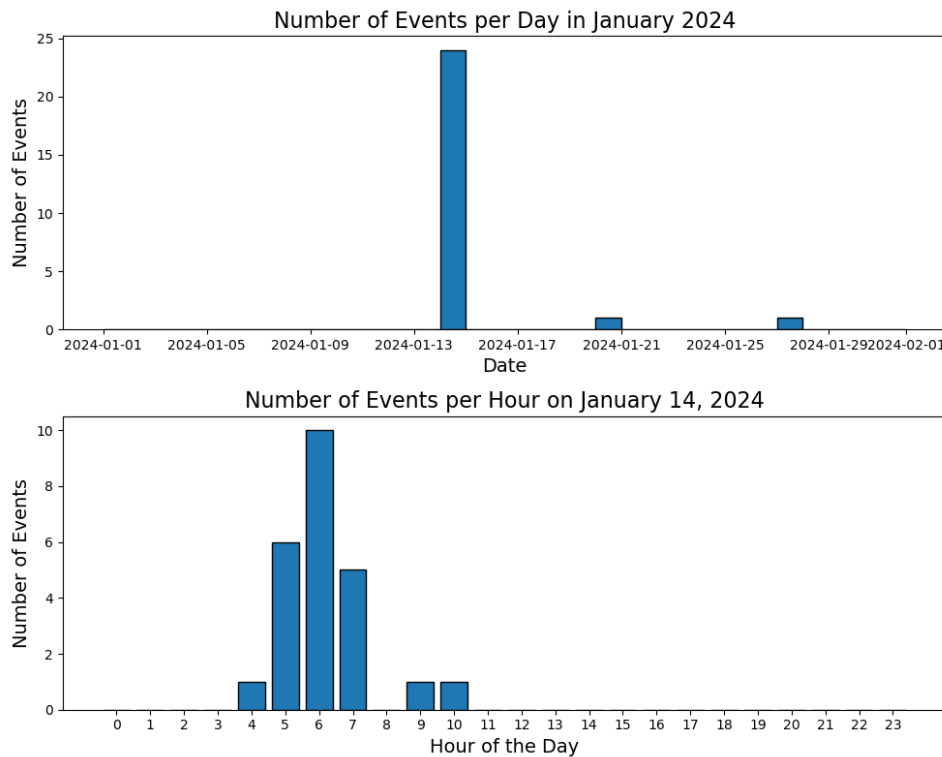


Figure 8: Histograms of the LP events distribution derived from the revised event catalog over the month of January 2024 (upper plot) with a focus of the distribution of LP events on the 14th of January (lower plot).

Given that the volcanic eruption took place at 7:57 UTC on January 14th, it is logical that the majority of events are clustered around this date. Interestingly, the events begin a few hours before the eruption and mostly subside shortly before 8:00. This pattern can be attributed to LP events, which are typically caused by the movement of fluids. Such movements include processes like bubble formation and collapse, or the flow of fluids into cracks or pipes (Sciotto et al., 2022).

The two events not occurring on January 14th are depicted in Figure 9. In Figure 9a, one of these events exhibits energy primarily up to 3 Hz, whereas the other events in the revised catalog generally extend up to just under 5 Hz. This difference may be attributed to the event occurring outside the eruption window, which spanned from January 14th to 16th, 2024, potentially resulting in less background noise

and fewer overlapping events. Conversely, the event shown in Figure 9b has a duration of approximately 40 seconds, significantly longer than the typical range of 8-12 seconds for other events. The seismogram for this event also reveals a possible secondary event emerging around 25 seconds, suggesting that the extended duration might be due to the presence of two or more overlapping LP events.

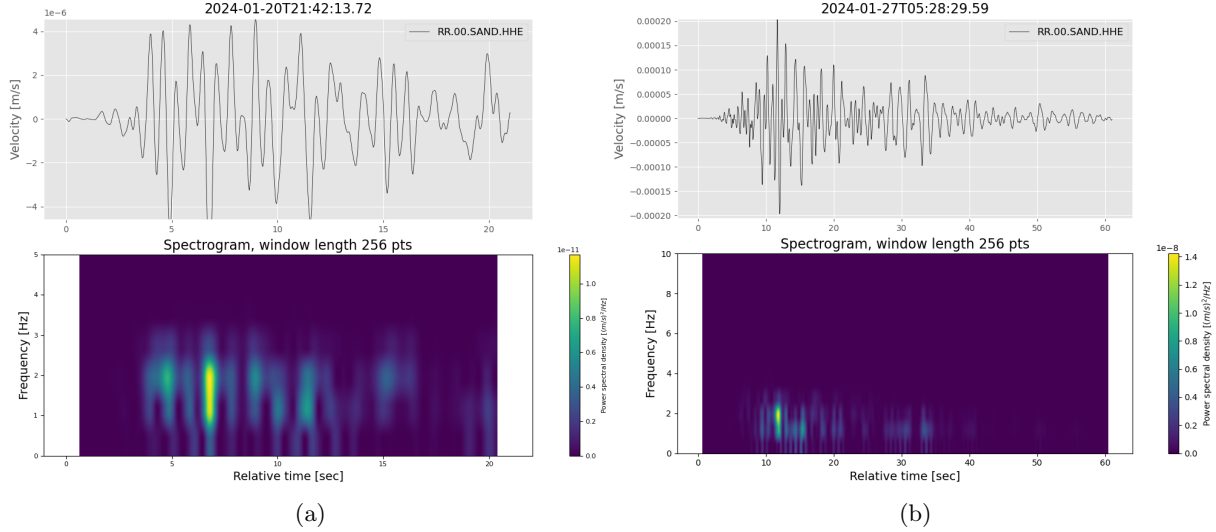


Figure 9: The seismogram (upper plot) and spectrogram (lower plot), both 0.5-5 Hz bandpass filtered, of the long-period events on the 20th (a) and 27th (b) of January, 2024.

By examining these histograms, we can gain insights into the temporal distribution of seismic events associated with the volcanic activity. The early onset of events prior to the eruption suggests pre-eruptive fluid movements, while the decline in events after the eruption indicates a reduction in such activities.

3.5 Cross Correlation

To verify the events in the revised event catalog, a further analysis using cross-correlation was conducted. For this analysis, a template event needed to be selected. The chosen event is from January 14th, 2024, at 06:28:59 UTC (see Figure 10). This specific event was selected because it occurred on January 14th, had minimal interference from other events, and exhibited low background noise.

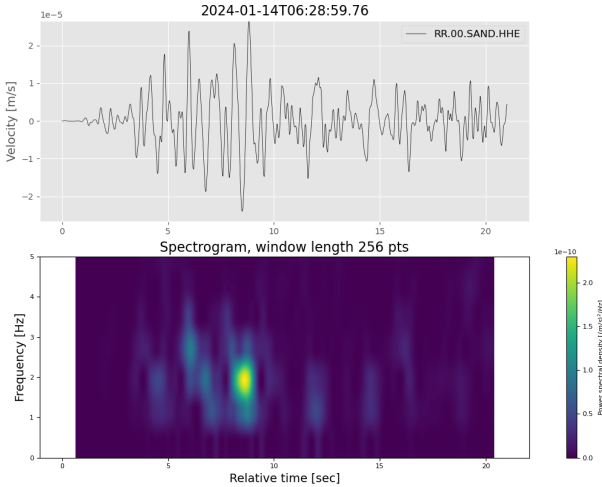


Figure 10: The seismogram (upper plot) and spectrogram (lower plot), both 0.5-5 Hz bandpass filtered, of the event used in the cross correlation as the template.

The selected event was then used to cross-correlate with the seismic data for the entire month. This process involves matching the chosen template event with similar patterns in the seismic data to identify and confirm other occurrences of similar events using Obspy (Beyreuther et al., 2010). The identified events were saved in an additional catalog, which comprises 39 events that are concentrated on January 14th and 15th (see Figure 11).

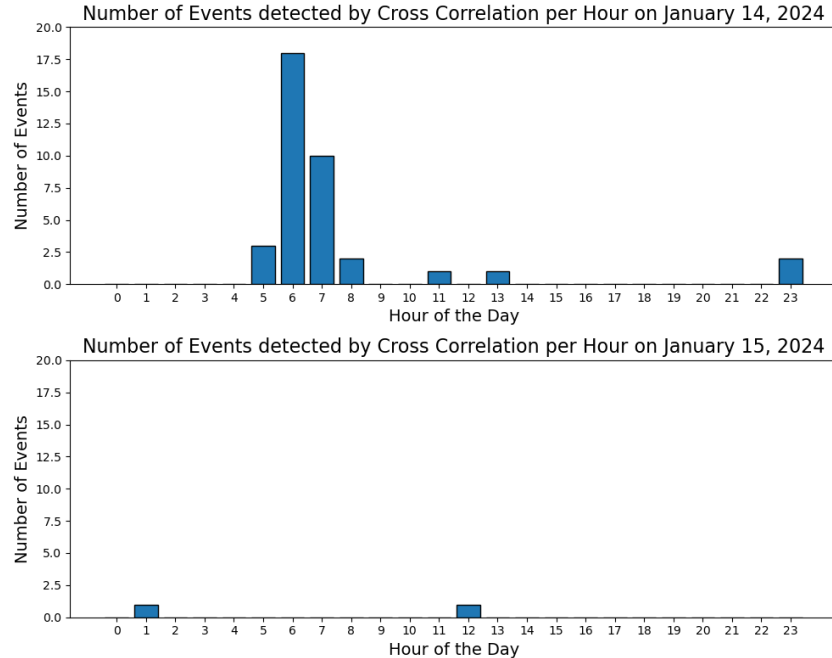


Figure 11: Histograms of the LP events derived from the cross correlation distribution over the 14th of January (upper plot) and on the 15th of January (lower plot).

This new catalog provides a more comprehensive understanding of the seismic activity associated with the volcanic eruption. By using cross-correlation, one can ensure that the identified events are consistent and accurately reflect the seismic activity. This method enhances the reliability of the event catalog and provides a clearer picture of the seismic patterns associated with the volcanic activity. While this method provides more events than the revised catalog has, these events have not been further analyzed. Conversely, looking at the temporal distribution of both catalogs, they share the result of most of the events being just before the start of the eruption indicating fluid movement within the volcanic system (see chapter 2).

This analysis highlights the temporal clustering of events and supports the hypothesis that these seismic activities are linked to the movement of fluids within the volcanic system. While this catalog contains further events the revised catalog used prior did not, other events are missing. However, both catalogs contain mainly events just before the start of the eruption with only a few events after the eruption started.

4 Results and Discussion

The analysis of seismic data from January 2024, recorded at stations SAND and SVA, focused on identifying and characterizing Long-Period (LP) seismic events associated with volcanic activity on the Reykjanes Peninsula.

The initial catalog of potential LP events, compiled using a bandpass filter ranging from 0.5 to 2 Hz, included 43 candidate events. Detailed analysis of these events' waveforms and frequency content reduced

this number to 27 confirmed LP events. Seismograms and spectrograms were crucial in distinguishing true LP events, characterized by energy concentrated in the lower frequency band (0.5-5 Hz). This analysis was conducted so events exhibiting significant energy in higher frequency bands could be excluded and only those with energy confined to the lower band were then considered true LP events.

A deeper understanding of the seismic events was achieved by examining the particle motion of the first second of the recorded signals. For instance, the particle motion analysis of a representative event from January 14, 2024, revealed complex looping patterns in the horizontal plane and elongated vertical motion, indicating significant contribution especially by the vertical component, indicating a vertically polarized wave as first arrival.

The direction of incoming seismic waves was further analyzed using rotational sensor data from the SVA station. By calculating the back azimuth of seismic events, it was determined that the seismic waves predominantly arrived from approximately 180 degrees, directly south of the SVA station, encompassing the area around Gríndavík and the fissures that opened in January 2024 and December 2023. Just before and after the event the backazimuth shifts to 240 degrees, meaning there is supposed to be a source in the South-West. This could potentially be background noise from the ocean or the Svartsengi and orbjörn area. This shift in back azimuth during the eruption further supports the localization of the seismic sources to the volcanic fissures in the region.

Temporal analysis of the LP events provided additional insights into the seismic activity's progression. Histograms illustrating the distribution of events over January 2024 showed a clear clustering around January 14th, coinciding with the onset of the volcanic eruption at 07:57 UTC. Notably, the majority of LP events began a few hours before the eruption and mostly subsided shortly afterward. This pattern is indicative of pre-eruptive fluid movements, such as bubble formation, collapse, and the flow of fluids into cracks or pipes, which are typical mechanisms for generating LP events.

Within the temporal analysis of the events, two events outside the main focus of events came to light that were different to the events in the 14th of January. The event on January 20 exhibited energy primarily up to 3 Hz, whereas the majority of other LP events in the revised catalog extended up to just under 5 Hz. This difference may be attributed to the event occurring outside the main eruption window, resulting in different background noise levels and fewer overlapping events. The event on January 27 had an unusually long duration of approximately 40 seconds, significantly longer than the typical range of 8-12 seconds for other events. The seismogram for this event also revealed a possible secondary event around 25 seconds, suggesting that the extended duration might be due to overlapping LP events or complex fluid dynamics occurring post-eruption.

To enhance the reliability of the identified LP events, cross-correlation analysis was performed using a well-defined template event from January 14th. This method identified 39 events, further confirming the temporal clustering around the eruption period. While the cross-correlation approach detected additional events not present in the initial catalog, it predominantly corroborated the concentration of seismic activity before the eruption. This analysis underscores the significance of pre-eruptive fluid dynamics in the lead-up to the volcanic eruption.

Overall, the comprehensive analysis of waveforms, particle motion, back azimuth, and temporal distribution provided a detailed characterization of the LP seismic events associated with the volcanic activity on the Reykjanes Peninsula. The findings highlight the critical role of fluid movements within the volcanic system in generating LP events and offer valuable insights into the seismic precursors of volcanic eruptions.

5 References

1. Beyreuther, M., Barsch, R., Krischer, L., Megies, T., Behr, Y., & Wassermann, J. (2010). ObsPy: A Python Toolbox for Seismology. *Seismological Research Letters*, 81(3), 530-533. <https://doi.org/10.1785/gssrl.81.3.530>

2. Chouet, B. A., & Matoza, R. S. (2013). A multi-decadal view of seismic methods for detecting precursors of magma movement and eruption. *Journal of Volcanology and Geothermal Research*, 1–10. Elsevier. <https://doi.org/10.1016/j.jvolgeores.2012.11.013>
3. Chouet, B. (1996). Long-period volcano seismicity: its source and use in eruption forecasting. *Nature*, 380, 309–316. <https://doi.org/10.1038/380309a0>
4. Heimann, S., Kriegerowski, M., Isken, M., Cesca, S., Daout, S., Grigoli, F., Juretzek, C., Megies, T., Nooshiri, N., Steinberg, A., Sudhaus, H., Vasyura-Bathke, H., & Willey, T. (2017). Pyrocko - An open-source seismology toolbox and library. GFZ Data Services. <https://doi.org/10.5880/GFZ.2.1.2017.001>
5. Icelandic Meteorological Office (IMO). (2024). Volcanic unrest in Grindavík. Vedur. <https://en.vedur.is/about-imo/news/volcanic-unrest-grindavik> (last visited July 16, 2024)
6. Mariangela Sciotto, A., Cannata, A., Di Grazia, G., & Montalto, P. (2022). Volcanic tremor and long period events at Mt. Etna: Same mechanism at different rates or not? *Physics of the Earth and Planetary Interiors*, 324. <https://doi.org/10.1016/j.pepi.2022.106850>
7. Troll, V. R., Deegan, F. M., Thordarson, T., Tryggvason, A., Krmíček, L., Moreland, W. M., Lund, B., Bindeman, I. N., Höskuldsson, Á., & Day, J. M. D. (2024). The Fagradalsfjall and Sundhnúkur Fires of 2021–2024: A single magma reservoir under the Reykjanes Peninsula, Iceland? *Terra Nova*, 00, 1–10. <https://doi.org/10.1111/ter.12733>
8. Wassermann, J. (2012). Volcano Seismology. In P. Bormann (Ed.), *New Manual of Seismological Observatory Practice 2 (NMSOP-2)* (pp. 1–77). Potsdam: Deutsches GeoForschungsZentrum GFZ. https://doi.org/10.2312/GFZ.NMSOP-2_ch13
9. Woods, J., Donaldson, C., White, R. S., Caudron, C., Brandsdóttir, B., Hudson, T. S., & Ágústsdóttir, T. (2018). Long-period seismicity reveals magma pathways above a laterally propagating dyke during the 2014–15 Bárarbunga rifting event, Iceland. *Earth and Planetary Science Letters*, 1–10. Elsevier. <https://doi.org/10.1016/j.epsl.2018.03.020>